Scale-dependent anisotropy of the ocean velocity field

Oleg Melnichenko (oleg@esr.org)

Earth and Space Research, Seattle WA

OSTST 2023

Abstract

The anisotropic structure of the ocean velocity field is re-examined using ~30 years of satellite altimetry observations, combined with results from a high-resolution ocean circulation model. In particular, we try to understand if the degree of anisotropy of the flow field is scale-dependent and how it varies in time. We find that low-frequency variations (periods longer than 16 months) are characterized by large positive values of the anisotropy coefficient indicating the dominance of zonal movements. The geographical distribution of the energy containing length scales of the low-frequency variability is similar to that of the eddy length scales (from the eddy dataset), suggesting that mesoscale eddies and, in particular, eddy movements project strongly on the low-frequency variability. Higher-frequency variability (periods shorter than 9 months) is primarily isotropic (except for a very narrow near-equatorial region) and characterized by generally shorter spatial scales varying from about 400 km wavelength near the equator to 100 km wavelength towards sub-polar latitudes. The Aviso fields show spurious negative anisotropy at short temporal and spatial scales, reflecting presumably correlated errors in sea level anomaly (SLA) maps. These effects are visible mostly in sub-tropical latitudes and the velocity variance at these scales is relatively low. Averaged over all time scales, the distribution of the flow anisotropy geographically and as a function of spatial scale provides a more nuanced view on the flow regimes. An example would be elevated zonal anisotropy on the northern and southern flanks of the Antarctic Circumpolar Current (ACC) associated with relatively long spatial scales and reduced zonal anisotropy along the core of the ACC at the mesoscale. Likewise, elevated levels of zonal anisotropy in the interiors of the subtropical gyres (particularly in their eastern parts) in the mesoscale range are mainly associated with the so-called "eddy trains" and/or "polarized eddy tracks". The effect of this kind of eddy anisotropy on the horizontal transport and mixing of tracers is assessed using numerical experiments with Lagrangian particle trajectories.

$\alpha = \frac{\langle u^2\rangle - \langle v^2\rangle}{\langle u^2\rangle + \langle v^2\rangle}$ - degree of anisotropy, evaluated in **frequency** (e.g., $\overline{u'u'} = \int_{\omega_1}^{\omega_2} Re[\hat{u}(\omega)\hat{u}^*(\omega)d\omega]$) or **wavenumber** domain.

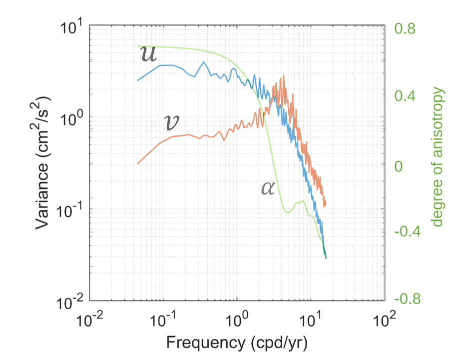

Frequency spectrum of velocity fluctuations (Aviso) in the area [156-164ºW,18-26ºN]

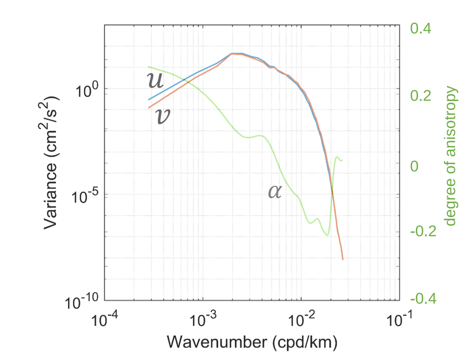

Wavenumber spectrum of velocity fluctuations (Aviso) in the area [154-170ºW,16-32ºN]

Numerical experiments with "virtual" particles are conducted in the eastern North Pacific and utilize altimetry-derived velocity fields. Particle trajectories are used to compute Lagrangian single-particle statistics (e.g., Rypina et al. 2012),

$$D_x = \frac{1}{N}\sum_{n=1}^{N}[x_n(t) - \bar{x}(t)], \quad D_y = \frac{1}{N}\sum_{n=1}^{N}[y_n(t) - \bar{y}(t)], \quad K_x = \frac{1}{2}\frac{\partial D_x}{\partial t}, \quad K_y = \frac{1}{2}\frac{\partial D_y}{\partial t},$$

where $x_n(t), y_n(t)$ are zonal and meridional displacements of particles from their initial positions and $\bar{x}(t), \bar{y}(t)$ are displacements of the center-of-gravity of a particle cloud.

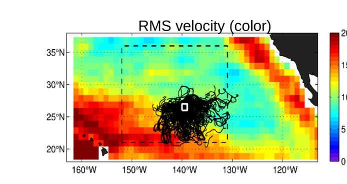

Examples of particle spreading over a period of 300 days. Initial locations are in the white rectangle. Background color shows RMS velocity (Aviso).

All time- (length-) scales together

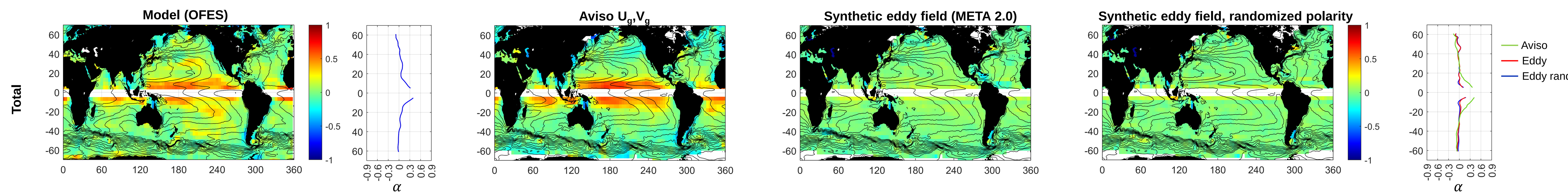

Integrated over all time- and length- scales, the ocean velocity field appears to be isotropic nearly everywhere (consistent with previous studies) except for a narrow near-equatorial region (15ºS-15ºN) dominated by the strongly anisotropic equatorial β-plane dynamics. The same is true for the synthetic eddy velocity field composed of contributions of perfectly isotropic Gaussian eddies but distributed in space and time as the observed mesoscale eddies in the eddy dataset (META 2.0). Overall, the eddy variability is isotropic as if eddies do not interact with the mean flow. Is it because the averaging is done over too long period of time mixing different dynamical regimes and/or eddy life cycles? Yet, if the eddy velocity field is isotropic, why is the eddy-induced material transport (diagnosed from the same velocity field) significantly anisotropic (e.g., Rypina et al. 2012)?

As a function of time-scale (frequency)

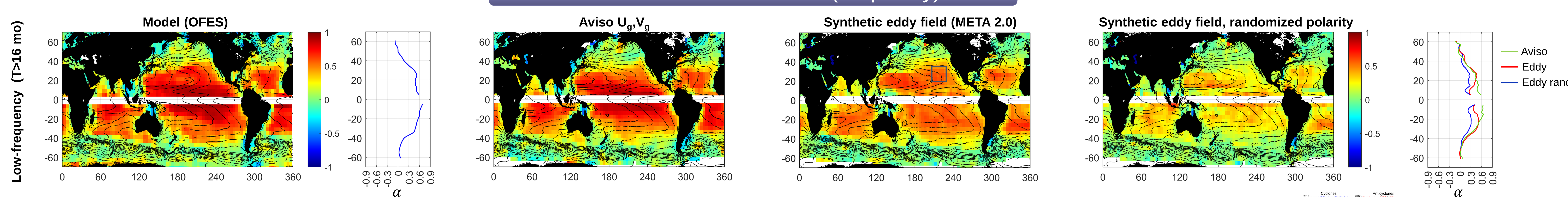

Low-frequency motions (periods longer than 16 months) are characterized by large positive values of the anisotropy coefficient particularly in the tropics and subtropics indicating the dominance of zonal movements. In the equatorial belt, this is due to long equatorial waves. In the subtropics, this is partly due to eddy east-west propagation (averaging over time T, $L_y = R_{eddy}$, while $L_x = R_{eddy} + C_pT$ (Huang et al., 2007)), but only partly. In significant part, strong zonal anisotropy in the subtropics is associated with the so-called structural anisotropy or eddy organization. Eddies are not completely random but organized into polarized "eddy trains" or "storm tracks". "Eddy trains" themselves are not stationary but slowly drift meridionally (see an example to the right).

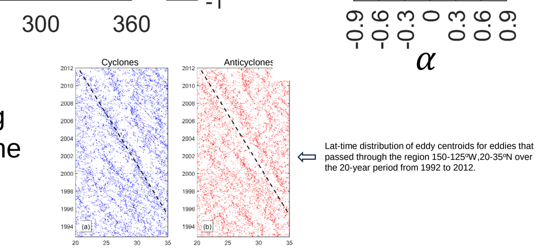

Lat-time distribution of eddy centroids for eddies that passed through the region 150-125ºW,20-35ºN over the 20-year period from 1992 to 2012.

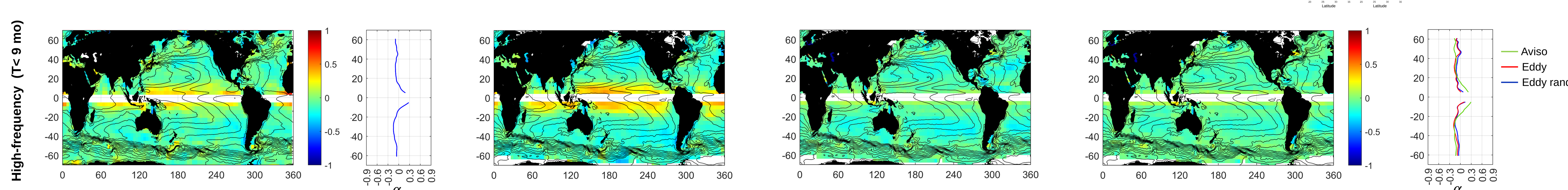

High-frequency variability (periods shorter than 9 months) is characterized by zero or very weak meridional anisotropy. The near-equatorial region with the strong anisotropic, equatorial β-plane dynamics is again an exception.

As a function of length-scale (wavenumber)

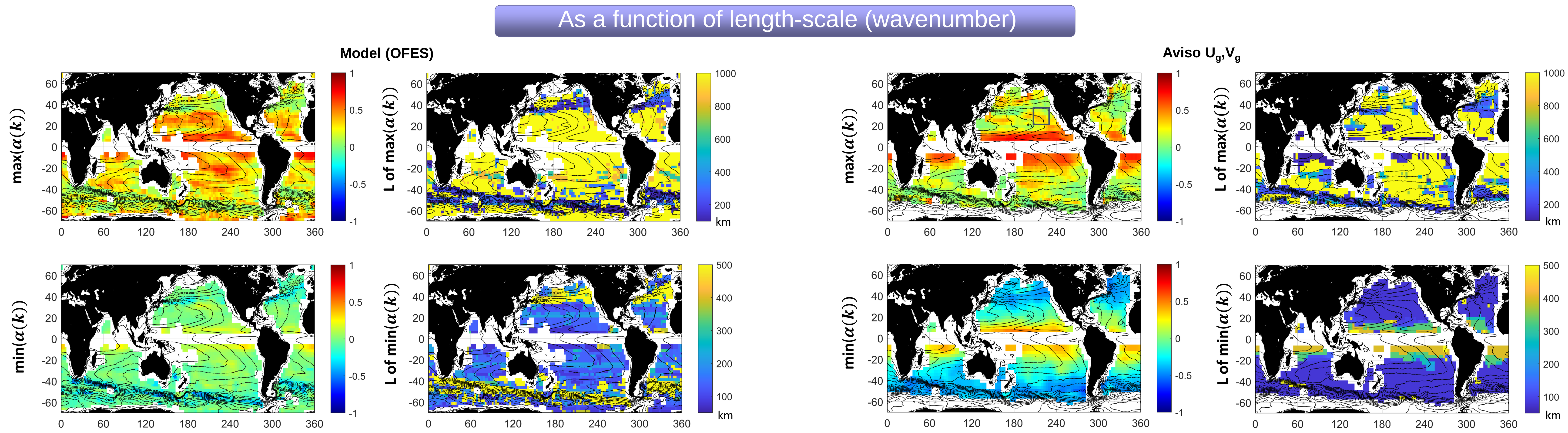

The distribution of the flow anisotropy geographically and as a function of the spatial scale shows a more nuanced view on the flow regimes. Elevated levels of zonal anisotropy are observed on the northern and southern flanks of all major currents, such as the Antarctic Circumpolar Current (ACC), the Gulf Stream and Kuroshio Extensions, etc. These features are associated with relatively long spatial scales. Reduced levels of zonal anisotropy are observed along the cores of these currents and are associated with the mesoscale. Likewise, elevated levels of zonal anisotropy in the mesoscale range are observed in the interiors of the subtropical gyres (particularly in their eastern parts) and are mainly associated with the so-called "eddy trains" and/or "polarized eddy tracks".

Implications for transport of tracers

The eddy-induced material transport is anisotropic simply because eddies move in the preferred direction. Eddies propagate westward; therefore, the eddy-induced transport is zonally anisotropic. (In principle, there is no need for "zonally elongated large-scale transients" (Kamenkovich et al. 2015) or any other types of anisotropic structures to induce anisotropic material transport). This can be explained using the same arguments used to explain the suppression of eddy mixing by strong zonal jets (Ferrari and Nikurashin, 2010). Indeed, following Klocker and Abernathey (2014) $K_y = \frac{K_0}{1+k^2\gamma^{-2}(C_x-U)^2}$, $K_x = \frac{K_0}{1+k^2\gamma^{-2}(C_y-V)^2}$ (K_0 - "unsuppressed" diffusivity, k – eddy length scale, γ – eddy decorrelation inverse time scale). If $(U,V) = 0$ (no background flow), $K_y < K_x$ simply because $C_y = 0$ and C_x is not.

Aviso velocity field

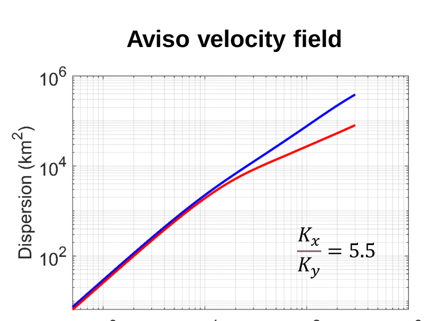

Synthetic eddy velocity field (META 2.0)

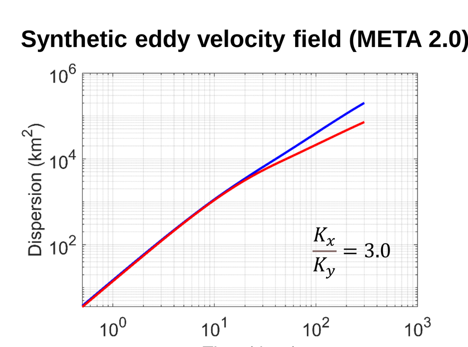

Synthetic eddy velocity field random locations, random propagation

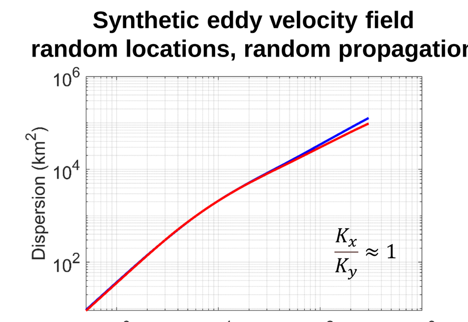

Particle dispersion in the zonal (blue) and meridional (red) directions for deployments in the area 152-130ºW, 21-37ºN. Estimates of the zonal and meridional components of Lagrangian diffusivity are made by fitting straight lines to dispersion curves over t from 182 to 300 days.

The effect of the eddy organization ("eddy trains") on the eddy-induced transport of tracers can be estimated by contrasting two synthetic eddy velocity field experiments. One is composed of eddies as they are in the eddy dataset (META 2.0), and the other is composed of the same eddies (locations, trajectories, amplitudes) but with randomized polarities (to break "eddy trains").

Synthetic eddy velocity field (META 2.0)

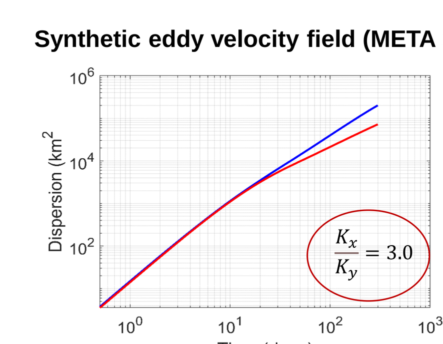

vs.

Synthetic eddy velocity field (META 2.0) randomized polarity

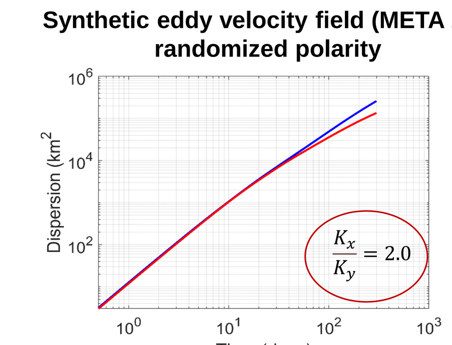

Particle dispersion in the zonal (blue) and meridional (red) directions for deployments in the area 152-130ºW, 21-37ºN in two experiments with synthetic eddy velocity fields.

References:
Chen, C., and I. Kamenkovich, 2016: Eddy trains and striations in quasi-geostrophic simulations and the ocean, *J. Phys. Oceanogr*., 46, 2807-2825.
Ferrari, R. and M. Nikurashin, 2010: Suppression of eddy diffusivity across jets in the Southern Ocean, *J. Phys. Oceanogr*., 40, 1501-1519.
Kamenkovich, I., I.I. Rypina, and P. Berloff, 2015: Properties and origins of the anisotropic eddy-induced transport in the North Atlantic, *J. Phys. Oceanogr*., 45, 778-791.
Klocker, A., and R. Abernathey, 2014: Global patterns of mesoscale eddy properties and diffusivity, *J. Phys. Oceanogr*., 44, 1030-1046.
Rypina, I.I., I. Kamenkovich, P. Berloff, and L. Pratt, 2012: Eddy-induced particle dispersion in the near-surface North Atlantic, *J. Phys. Oceanogr*., 42, 2206-2228.

Acknowledgements:
This research was supported by NASA OSTST grant 80NSSC21K1739.
The processing and distribution of the Sea Level Anomaly (SLA-H), Absolute Dynamic Topography (ADT-H) Heights and Geostrophic Velocities (SLA-UV and ADT-UV) products are made by the Copernicus Marine Environment Monitoring Service (CMEMS).
The altimetric Mesoscale Eddy Trajectories Atlas (META2.0) was produced by SSALTO/DUACS and distributed by AVISO+ (https://aviso.altimetry.fr) with support from CNES, in collaboration with IMEDEA .
The OFES simulation was conducted on the Earth Simulator under the support of JAMSTEC (Data DOI: https://doi.org/10.17596/0002029)